



Citation: A. Crespi, A. Borghi, A. Facchi, C. Gandolfi, M. Maugeri (2020) Spatio-temporal variability and trends of drought indices over Lombardy plain (northern Italy) from meteorological station records (1951–2017). *Italian Journal of Agrometeorology* (2): 3-18. doi: 10.13128/ijam-1101

Received: September 30, 2020

Accepted: November 14, 2020

Published: January 25, 2021

Copyright: © 2020 A. Crespi, A. Borghi, A. Facchi, C. Gandolfi, M. Maugeri. This is an open access, peer-reviewed article published by Firenze University Press (<http://www.fupress.com/ijam>) and distributed under the terms of the Creative Commons Attribution License, which permits unrestricted use, distribution, and reproduction in any medium, provided the original author and source are credited.

Data Availability Statement: All relevant data are within the paper and its Supporting Information files.

Competing Interests: The Author(s) declare(s) no conflict of interest.

Spatio-temporal variability and trends of drought indices over Lombardy plain (northern Italy) from meteorological station records (1951–2017)

ALICE CRESPI^{1,a,*}, ANNA BORGHI^{1,b}, ARIANNA FACCHI¹, CLAUDIO GANDOLFI¹, MAURIZIO MAUGERI^{2,3}

¹ Department of Agricultural and Environmental Sciences, Università degli Studi di Milano, Milan, 20122, Italy

² Department of Environmental Science and Policy, Università degli Studi di Milano, Milan, 20122, Italy

³ Institute of Atmospheric Sciences and Climate, National Research Council, Bologna, 40129, Italy

^a Now at Institute for Earth Observation, Eurac Research, Bolzano, 39100, Italy

^b Now agronomic consultant, via Costa d'Oro 8, Cernobbio, 22012, Italy

*Corresponding author. E-mail: alice.crespi@eurac.edu

Abstract. A 30-arc second resolution gridded dataset of 1951–2017 monthly series of Standardized Precipitation Index (SPI) and Standardized Precipitation Evapotranspiration Index (SPEI) for a portion of Po Plain in Lombardy region (northern Italy) is presented. The series were derived from an archive of homogenized and quality-checked meteorological station observations covering the study area and its surroundings, which were interpolated onto regular grid by means of an anomaly-based procedure. A significant negative trend in mean regional SPI series was depicted for summer (-0.14 decade⁻¹) while stronger decreases were found for SPEI in spring, summer and year (-0.14 , -0.22 and -0.17 decade⁻¹, respectively). The greatest drying tendencies occur in the southern and western parts of domain where summer index trends reached -0.23 and -0.30 decade⁻¹, respectively. The more negative trends of SPEI than SPI can be probably explained by the increasing role of evapotranspiration over recent decades triggered by arising temperature. The assessment of spatio-temporal variability of drought features (frequency, duration and severity) pointed out increasing tendencies in all cases, especially in the western portion of the region.

Keywords. SPI, SPEI, trend analysis, drought, Po Plain.

INTRODUCTION

Drought is a weather and climate-related natural hazard referring to a temporary scarcity of natural water availability due to a prolonged rainfall deficit, which could affect a wide range of environmental, social and economic systems, such as food production and agriculture (Parsons et al., 2019; Vicente-Serrano

et al., 2012). Several definitions are currently used to classify the different kinds of drought and their impacts; in particular, meteorological droughts refer to the reduction of precipitation with respect to normal conditions over a specific period and region (Spinoni et al., 2014). Although several studies provided evidences that globally land areas in very dry conditions have enlarged over the last decades (Spinoni et al., 2018; Dai et al., 2004) and a general increase of extreme events in the context of global warming is expected (IPCC, 2014), drought behavior exhibits a high variability at both temporal and spatial scales. In Europe spatial differences were clearly depicted with a tendency to wetter conditions in the North-East and to drier regimes in the South, especially in Mediterranean areas, enhanced by lower precipitation together with increasing evapotranspiration fostered by higher temperature (Spinoni et al., 2015; Briffa et al., 2009). However, since drought variations could be even greater at sub-regional and local levels, the reconstruction of the recent climate evolution at high spatial resolution from dense meteorological networks is crucial to analyze local trends and to define water management plans and future adaptation strategies. Moreover, in order to provide a more comprehensive drought characterization and to define its effects on natural and managed systems dependent on water supply, it is necessary to consider not only precipitation, which is the main driver of drought, but also the role of temperature influencing evapotranspiration variability and thus drought severity (Vicente-Serrano et al., 2014). This could be particularly relevant for Mediterranean regions, which are some of the main hotspots in the context of global warming (Founda et al., 2019; Lionello and Scarascia, 2018).

In Italy, recent studies focused on the analysis of drought frequency and intensity variations over several central and southern regions by computing different drought indices from station observations (Vergni and Todisco, 2011; Piccarreta et al., 2004). These studies agreed in depicting a general increase of drought events and their duration over recent decades, even though the intensity of such phenomena depends both on spanned period and temporal resolution, and it is strongly influenced by orographic heterogeneity (Buttafuoco et al., 2015; Di Lena et al., 2014). Less studies dealt with drought characterization for northern Italian regions (Baronetti et al., 2020; Brunetti et al., 2009) and a general positive tendency in drought occurrence was depicted, which became more evident during the most recent decades (Stagge et al., 2017).

The Po river plain is a large alluvial plain in northern Italy characterized by being one of the most important agricultural areas in Europe; consequently, it represents a very interesting study domain, where accurate information about the spatial variability of meteorologi-

cal variables could represent an essential support for the development and implementation of water management adaptation strategies. Agriculture in the Po plain is in fact largely dependent on irrigation and, therefore, it is strongly influenced by droughts.

In this framework, we reconstructed and analyzed the spatio-temporal trend and the variability of droughts over a portion of Po Plain (9°12'-10°30'E and 45°00'-45°45'N), computing the 1951–2017 monthly series of Standardized Precipitation Index (SPI, McKee et al., 1993) and of Standardized Precipitation Evapotranspiration Index (SPEI, Vicente-Serrano et al., 2010) starting from a dense database of historical precipitation and temperature records recovered for the study region and surrounding areas. All the data were checked for quality and homogeneity, and they were interpolated onto a 30-arc second resolution grid covering the study area in order to provide regional SPI and SPEI records and to assess drought indicator variability and hotspot locations at fine scale over the domain. Long and short-term trends in SPI and SPEI records were in fact investigated at both regional and local scales by considering two aggregation intervals (3 and 12 months) and the spatio-temporal evolution of the main features of drought spells, i.e. frequency, intensity and duration, was analyzed throughout the spanned period 1951–2017.

MATERIALS AND METHODS

Study area and meteorological database

The area considered for the present study is located in the middle of northern Italy and it includes a large portion of southern Lombardy and the northernmost part of Emilia-Romagna for a total of about 8500 km² (9°12'-10°30'E and 45°00'-45°45'N, rectangle in Fig. 1). The domain is centered on the lower part of the basin of Adda river, one of the main tributaries of Po river, and is characterized by a flat and homogeneous orography except for the northern part, where the first reliefs of pre-Alps occur.

Despite the presence of large urban centers such as Milan, Brescia and Bergamo, agriculture activities are intensively practiced with about 70% of the surface covered by irrigated crops, mainly maize and pasture. Very high crop productivities are achieved through an extensive development of irrigation, which relies on the water conveyed by a dense channel network and supplied by the main rivers.

The database used to assess the drought variability over the study domain was composed by more than 200 monthly precipitation series and 20 monthly maximum and minimum temperature series. The records were retrieved from the networks of regional services (ARPA

Lombardia, ARPA Emilia-Romagna, ARPA Veneto, ARPA Piemonte), the historical archives of the former Italian Hydrographic Service and several past projects focused on the recovery and homogenization of secular Italian meteorological series, especially RICLIC (<http://www.riclic.unimib.it/>) and NextData (<http://www.nextdataproject.it/?q=en>) projects.

In particular, the precipitation series were extracted from the quality-checked and homogenized database presented by Crespi et al. (2018a) where it was used to reconstruct the secular precipitation record over the upper Adda river basin.

The quality-check procedures included outlier detections and spatial consistency tests, in which each monthly series was reconstructed by means of the surrounding stations and the comparison between simulated and observed values allowed to detect suspicious entries, low-quality sites or periods of station malfunction. The same quality-check procedures were applied to temperature data and whenever the homogenized version was not already available, series homogeneity was controlled by means of a procedure based on the Craddock test (Craddock, 1979). In such method, for each test series several surrounding reference stations were selected and the series of cumulative differences between the test and each reference were computed and used to identify potential breaks. Inhomogeneous periods in the test series were corrected by applying proper correcting factors (Golzio et al., 2018). Relevant breaks were finally identified and the homogenization was performed for 8 minimum and maximum temperature series. After these activities the monthly mean temperature records were obtained as the average of maximum and minimum monthly values. The checked and homogenized dataset of station records was then used to project the meteorological records onto the 30-arc second resolution grid covering the study area.

Even though several series spanned a longer period in the past, the start of study period was set to 1951, when the availability of meteorological records significantly improved and the station distribution over the domain started to be more homogeneous. Although the coverage of temperature series is significantly less dense than that of precipitation data (Fig. 1), this it is not expected to affect result robustness thanks to the greater spatial coherence of temperature (Brunetti et al., 2006), which is particularly favored by the homogeneous orography of the domain. In addition, in the interpolation framework (see the next section for details on the interpolation method) the 20 monthly temperature series were integrated by the 1961–1990 climatological normals, i.e. the 30-year averages, of 125 sites included in the study domain and adjacent areas and retrieved from the database set up by Brunetti et

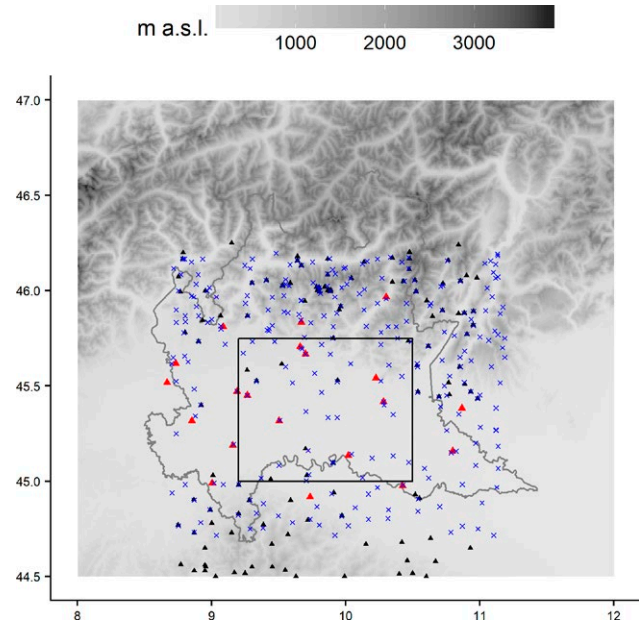


Fig. 1. Study domain (rectangle) and station distribution: blue crosses are precipitation sites, red triangles represent the locations of temperature series, while the black triangles indicate the sites for which 1961–1990 monthly temperature normals were considered.

al. (2014) for the construction of Italian temperature climatologies.

Data interpolation and SPI and SPEI calculation

The gridded datasets of 1951–2017 monthly meteorological records over the study domain were computed by applying the anomaly method (see e.g. New et al., 2001; Brunetti et al., 2012; Isotta et al., 2014). Specifically, the final precipitation and mean temperature grids were obtained by superimposing fields of long-term means of reference, i.e. the 30-year climatologies, and fields of anomalies, i.e. the departures from the reference values. The main advantage of the anomaly method is that it produces fields that are not biased by an uneven station distribution (New et al., 2001; Mitchell and Jones, 2005).

For both temperature and precipitation, 1961–1990 was used as reference period and the monthly normals were computed after filling the missing values in this 30-year interval by means of the procedure described in Crespi et al. (2018b). The normal interpolation over a 30-arc second resolution Digital Elevation Model (DEM, GTOPO30) was then performed by applying a local weighted linear regression of temperature (precipitation) *versus* elevation (Daly et al., 2002; Brunetti et al., 2014; Crespi et al., 2018b). The station weights entering in the fit were locally defined

on a monthly basis accordingly with their distance and orographic similarity to the cell to evaluate. For precipitation only, DEM was smoothed in order to account for the actual spatial scales at which the orography-atmosphere interactions are expected to occur (Foresti et al., 2018).

The station monthly series were then converted into anomalies by the difference (for temperature) and the ratio (for precipitation) from the corresponding normals. The anomalies were interpolated over the same grid by means of a weighted averaging approach with station weights depending on distance and elevation difference from the target cell and their decay was regulated on a yearly basis accordingly with the variation in station density over the study period. In particular, the distance halving coefficient was set year-by-year to the mean radius over the grid including at least three available data. The 1951–2017 monthly series in absolute values were finally computed by adding (multiplying) the gridded temperature (precipitation) anomalies to (times) the gridded climatologies. The accuracy of interpolated data was evaluated by means of the leave-one-out reconstruction of station data and the comparison with corresponding observations in terms of BIAS, Mean Absolute Error (MAE) and Root Mean Square Error (RMSE).

SPI and SPEI were computed both at cell level from the interpolated 1951–2017 meteorological series and at regional level from the areal mean of the gridded temperature and precipitation datasets over the domain. The standardized indices were computed by fitting the observation data with the Gamma probability distribution for SPI and the Log-logistic probability distribution for SPEI over the whole analyzed period (1951–2017). The chosen fitting distributions were proved to be the most suitable for SPI and SPEI computation, respectively, and are the mostly adopted in literature (see e.g. Beguería et al., 2014; Stagge et al. 2015).

While SPI (McKee et al., 1993) takes into account precipitation only, SPEI (Vicente-Serrano et al., 2010) is based on the difference between precipitation and potential evapotranspiration (PET). Several methods can be adopted to evaluate PET, with different requirements in terms of variables that need to be measured. Therefore, the choice largely depends on data availability and, even though more comprehensive methods, like Penman-Monteith's one (Allen et al. 1998), could provide more reliable PET estimation, in this work we applied the Thornthwaite's equation (Thornthwaite, 1948), since it requires only mean temperature values and it is particularly useful for long-term reconstruction if no or very few observations of other variables, such as vapor pressure or wind speed, were available in the past.

Negative SPI and SPEI values for a certain time step indicate drier regimes, i.e. less precipitation and/or greater

deficit, with respect to the mean conditions extracted from the whole period, whereas positive values of the indices highlight wetter conditions than reference mean values.

SPI and SPEI were computed at monthly resolution and for two aggregation intervals (3 and 12 months), in order to highlight the variability of climatic signal in relation to the integration periods and to assess the time scales at which the variations are mostly significant.

The 3 and 12-month aggregation interval records (named thereafter SPI (SPEI) -3 and SPI (SPEI) -12, respectively) were used to define seasonal and annual series. Specifically, seasonal series were defined by considering SPI (SPEI) -3 values in February for winter, May for spring, August for summer and November for autumn, while the annual ones were set up by selecting the SPI (SPEI) -12 values in December for each year.

In this work, long-term trends and significance of time series were evaluated by means of Theil-Sen (TS; Theil, 1950; Sen, 1968) and Mann-Kendall (MK; Kendall, 1975) tests.

RESULTS

The study area is characterized by temperate climatic conditions with the lowest 1961–1990 mean temperature in winter around +3 °C as average and the highest normals in summer when mean temperature values are around +22 °C. The lowest temperatures are depicted over the north-eastern part of the domain where the elevation gradients are higher, while the greatest temperature values characterize the southern part, close to the Po river. As regards the precipitation regime, no relevant seasonal differences occur and, except for winter when the minimum of precipitation is reached (180 mm), the average precipitation is around 250 mm in all seasons. The altitudinal gradient is well depicted also for precipitation distribution: the highest precipitation values occur over the northern part of the domain in correspondence of the beginning of pre-Alpine belt, where total precipitation is in some areas two times greater than the amounts characterizing the plain areas in the central and southern portions of domain. On yearly basis, total precipitation values reach 1500 mm in the North while the plain areas feature minima of less than 800 mm.

The errors on climatological fields were computed by the leave-one-out reconstruction of all station normals within the study area. The monthly mean absolute errors, as average over all stations, range between 7.9 and 14.8 mm for precipitation and between 0.7 and 0.8 °C for temperature.

The assessment of trends and variability in hydrological regime over the study domain was performed for the

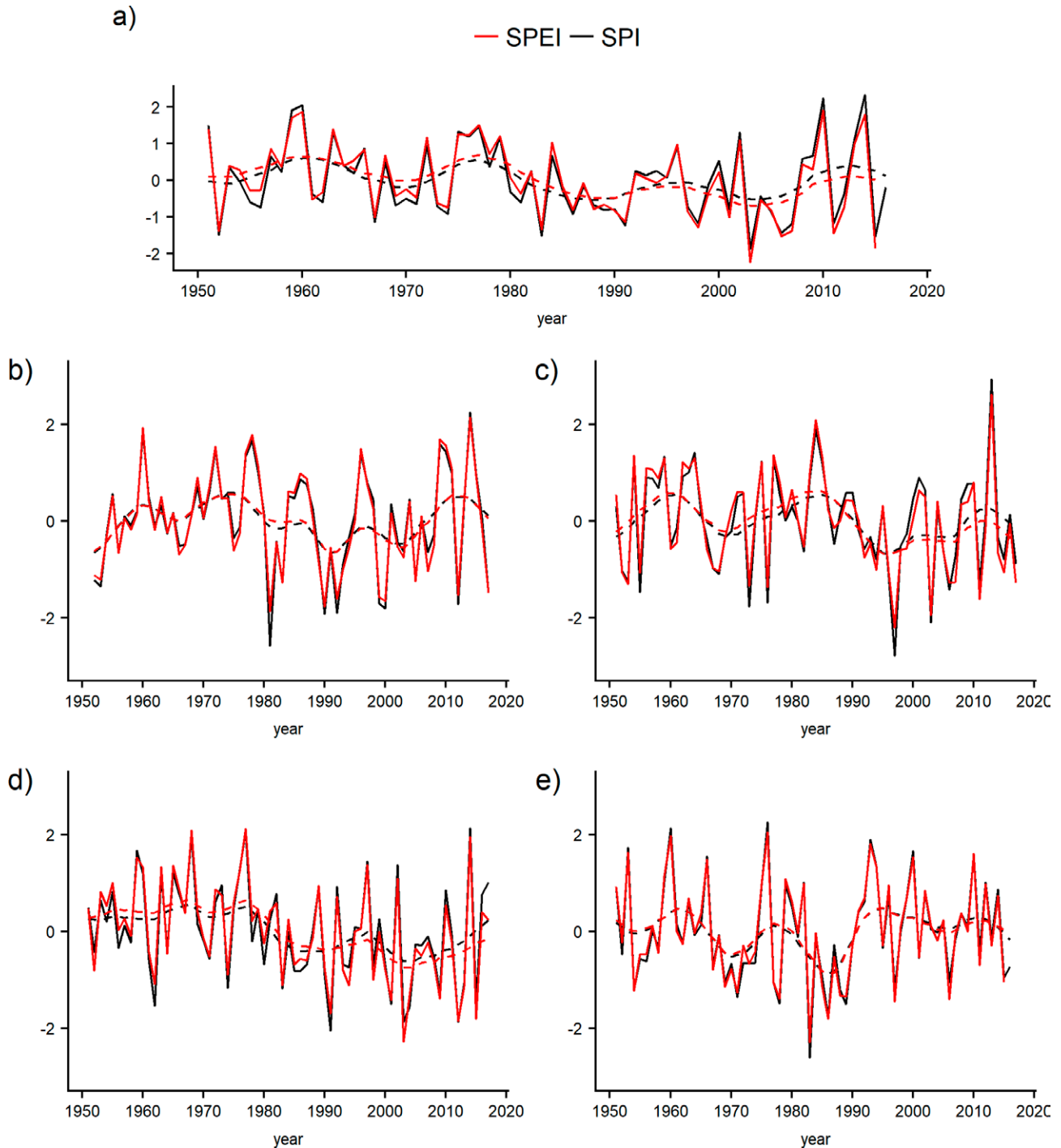


Fig. 2. 1951–2017 a) annual, b) winter, c) spring, d) summer and e) autumn SPI (black line) and SPEI (red line) obtained as average over all the grid cells of the study domain. The dashed lines represent the 11-year centred Gaussian filter with 3-year standard deviation of SPI (in black) and SPEI (in red) series.

1951–2017 period at both seasonal and annual scales. At this aim, the areal 1951–2017 monthly series of precipitation and deficit, i.e. the difference between precipitation

and PET, were defined by averaging the values estimated at all cells of the 30-arc second resolution grid and they were used to reconstruct the corresponding SPI and SPEI series

over the whole spanned period. The series are displayed in Fig. 2. Autumn and annual values were not computed in 2017 for both indices due to the end of precipitation records in October 2017 and in 2016 for SPEI only due to the lack of available temperature observations in November 2016.

In the series of both indices, the driest year was 2003, which was characterized by a dry spell in summer (panels a) and d) in Fig. 2) when exceptional temperature values (mean areal temperature anomaly of +4.3 °C in respect with 1961–1990 summer normals) were combined with low precipitation (mean areal precipitation anomaly of 0.5 in respect with 1961–1990 summer normals). The wettest year was 2014 when total precipitation amounts exceeded normals, especially in summer (panels a) and d) in Fig. 2) with a precipitation anomaly of about 1.7 in respect with the corresponding 1961–1990 mean value. High annual index values were also registered in 2010 when the main contribution was provided by winter precipitation (panels a) and b) in Fig 2), which reached a seasonal areal anomaly of 1.7.

The TS slopes obtained for the 1951–2017 areal SPI and SPEI series at seasonal and annual scales are listed in Tab. 1. As regards SPI, the values experience negative tendencies, i.e. drying trends, in spring, summer and at annual scale, while winter and autumn are characterized by slight index increases, i.e. wetting tendencies. All resulting trends are not statistically significant with MK p-value above 0.05, except for summer, when the greatest SPI decay occurs and it is around $-0.14 \text{ decade}^{-1}$. The trends of SPEI index show similar results, however in this case the TS slopes are more negative in summer, spring and at annual scale and all these three values turned out to be statistically significant. The stronger signal provided by SPEI index could be explained by the increasing role of evapotranspiration driven by a positive and significant mean annual temperature trend of about $+0.3^\circ\text{C decade}^{-1}$ over the period.

In order to further analyze the evolution of drought indices over shorter time scales, the running trend of seasonal and annual SPI and SPEI series was computed. TS

trend and MK test were performed over moving windows of increasing length from a minimum of 20 years to the total length of the series and spanning all the 1951–2017 period. The results of the running trend are reported in Fig. 3 and Fig. 4 for the seasonal SPI and SPEI series, respectively, and Fig. 5 for annual values. The significant long-term trends of seasonal and yearly SPI and SPEI series, i.e. computed over the total length of the series, which were already discussed in Tab. 1, were also confirmed in the running-trend results (Fig. 3, Fig. 4 and Fig. 5). Besides the long-term trends, significant tendencies occurring over shorter time intervals are highlighted. It is interesting to note that SPEI series exhibit more relevant trends than SPI values at both long and short-time scales. In particular, a tendency towards drier conditions over time windows of 20–30 years are pointed out for spring and summer (panels b) and c) in Fig. 4) for intervals starting between 1970 and 1990 and between 1960 and 1980, respectively.

In addition to the regional behavior, the 1951–2017 seasonal and annual trends in SPI and SPEI series were also computed for each cell of the 30-arc second resolution grid in order to assess the spatial distribution of drought variability.

As regards the seasonal analysis, grid cells with significant trends were found out in summer for SPI (panel d) in Fig. 6) and in summer and spring for SPEI (panels c) and d) in Fig. 7).

Spring and summer trends are both negative over the whole domain and statistical significance occurs for all cells for SPEI in summer, while for the SPI gridded dataset no signal is depicted for spring, and in summer the negative trends with MK p-values below 0.05 occur over less than half study region. It is worth noting that both indices suggest a more relevant drying tendency in the southern and the western parts of the domain where SPEI summer trends reach $-0.30 \text{ decade}^{-1}$ and SPI ones are slightly lower and around $-0.23 \text{ decade}^{-1}$. In winter and autumn trends show MK p-values much greater than 0.05 in all cases, however the spatial patterns of TS slopes are comparable with spring and summer distributions: values are negative in the south-western part of region, even though much less pronounced, while decreasing tendencies occur in the north-eastern portion of the study area.

At annual scale, SPI and SPEI trends are negative over the whole region, with significant slopes located in the western, for SPI, and south-western, for SPEI, portions of the area (panel a) in Fig. 6 and Fig. 7).

As further analysis, SPI-3 and SPEI-3 gridded indices were used to evaluate the spatial distribution and temporal variability of some specific drought indicators. We considered the frequency, duration and severity of drought events, choosing a 3-month temporal aggregation since it

Tab. 1. Trends of SPI and SPEI series over 1951–2017 for winter (DJF), spring (MAM), summer (JJA), autumn (SON) and year. TS slopes are reported only if the trend is statistically significant (MK p-value < 0.05), otherwise trend sign is indicated. Trends are expressed as variation per decade.

	SPI	SPEI
DJF	+	-
MAM	-	-0.14
JJA	-0.14	-0.22
SON	+	+
YEAR	-	-0.17

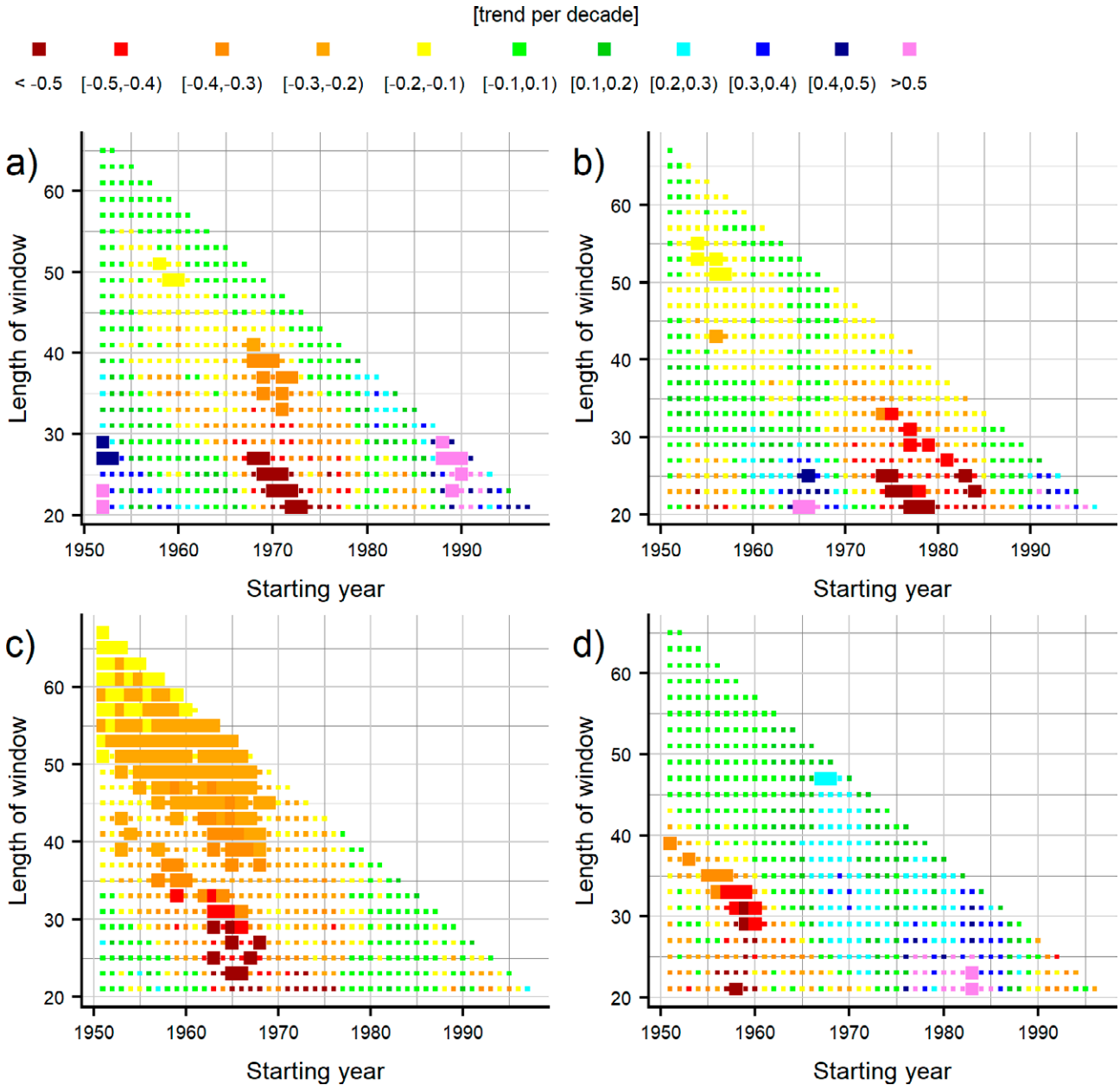


Fig. 3. Running trend analysis on SPI seasonal series: a) winter (DJF), b) spring (MAM), c) summer (JJA), d) autumn (SON). Colors represent the value of the TS slope while pixel thickness depends on the MK trend significance: pixels corresponding to MK p-values below 0.05 are reported with greater size. On the y-axis the length of the window is reported in terms of number of years.

is expected to be a suitable scale to describe drought affecting vegetation and agricultural practices (Bordi et al., 2007). For six subsequent decades from 1951 to 2010, the drought events were identified by following the definition of McKee (1993), i.e. a drought episode starts in the month (included) when the index value falls below -1 and ends in the month (not included) when the value returns positive, for at least two consecutive months. In particular, for each

subperiod we computed the drought frequency (DF) as the total number of identified drought spells in the decade, the total drought duration (TDD) as the total number of months included in the events and the total drought severity (TDS) as the sum (dimensionless) of the absolute values of the integral areas under the index curve from the start to the end month of each drought spell (Spinoni et al., 2015). In the following, only the outcomes from SPEI-3 se-

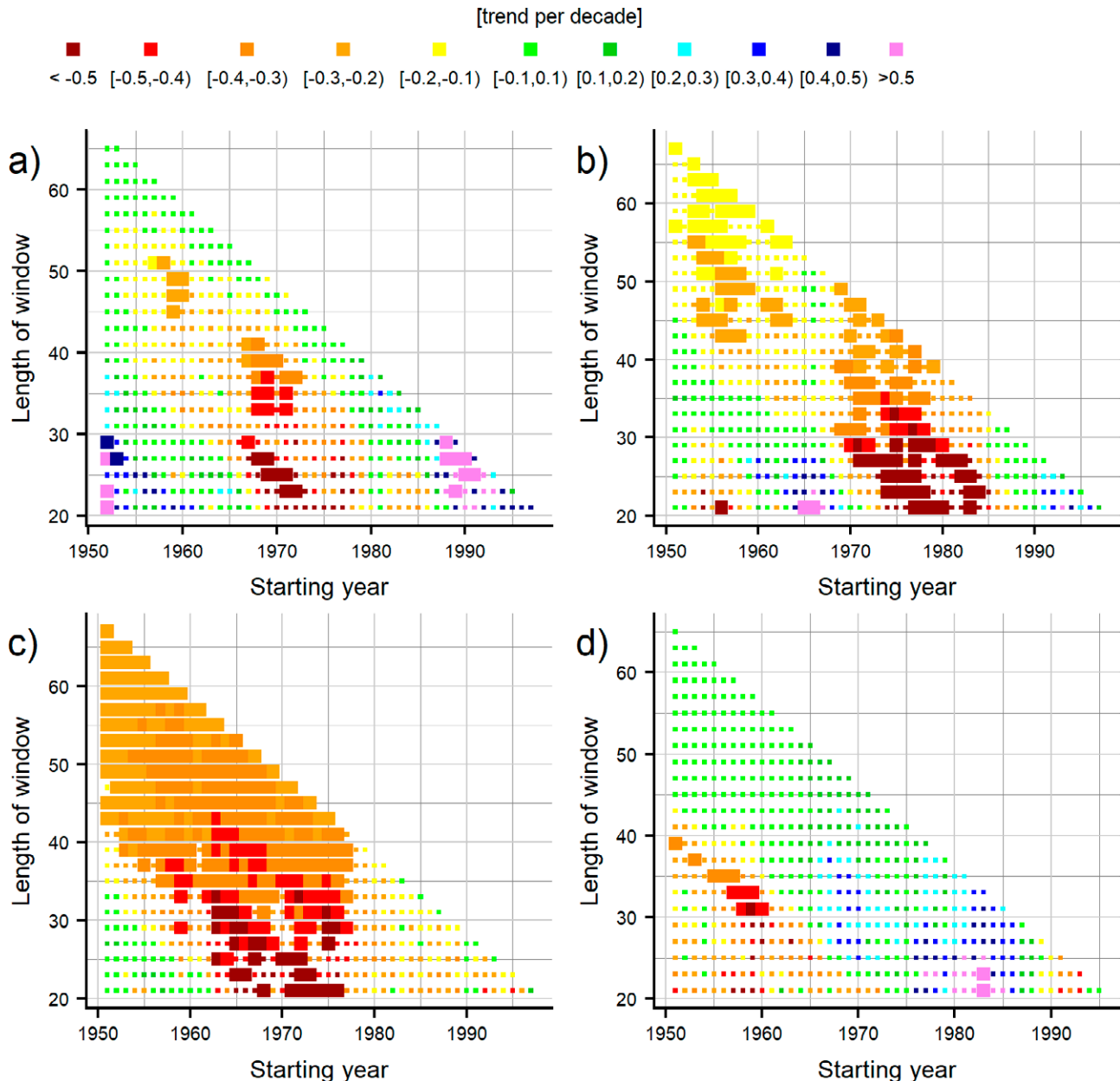


Fig. 4. Running trend analysis on SPEI seasonal series: a) winter (DJF), b) spring (MAM), c) summer (JJA), d) autumn (SON). Colors represent the value of the TS slope while pixel thickness depends on the MK trend significance: pixels corresponding to MK p-values below 0.05 are reported with greater size. On the y-axis the length of the window is reported in terms of number of years.

ries are discussed and shown, since SPI-3 exhibits a similar behavior, but with a weaker signal, as also pointed out by the long-term trend analyses.

The spatial distribution of the gridded indicators over the six subsequent decades (Figs. 8-10) highlights in all cases higher values from the decade 1981–1990 onwards in respect with the previous decades. The total number of drought spells that occurred over each one of the first three

decays was lower than 11 over the whole domain (panels in the top row of Fig. 8), while the number of drought events per decade was in the range of 11–17 in the following 10-year intervals (panels in the bottom row of Fig. 8). A similar increasing behavior was depicted for TDD and TDS: the total number of months experiencing drought conditions and the total severity of the drought events passed, as averages over the study domain, from 32 months and

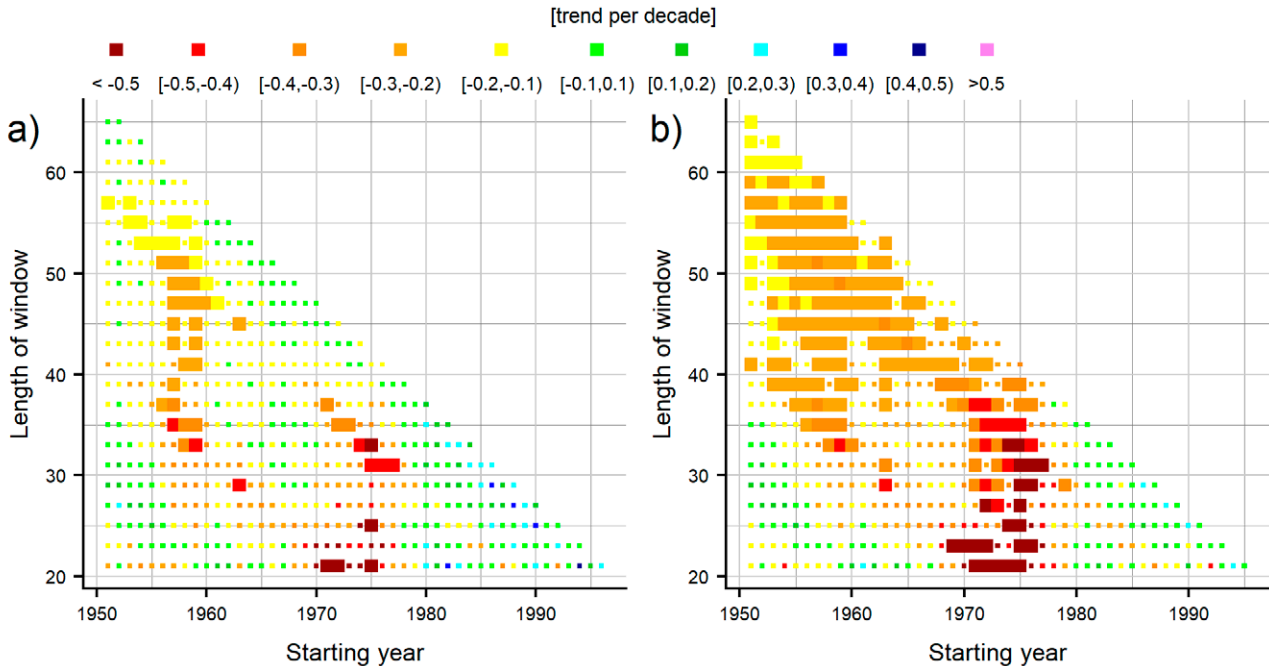


Fig. 5. Running trend analysis on SPI (left panel) and SPEI (right panel) annual series. Colors represent the value of TS slopes while pixel thickness depends on the MK trend significance: pixels corresponding to MK p-values below 0.05 are reported with greater size. On the y-axis the length of the window is reported in terms of years.

29 scores in 1951–1990, respectively, to 71 months and 72 scores in 2001–2010.

The 6-point series of DF, TDD and TDS for each grid cell were then subjected to a linear trend analysis. It is worth to note that this analysis, although the robustness of the results is limited by the small number of values, allows to provide a preliminary description of the inter-decadal variability of drought features as well as of its spatial distribution over the study domain. The spatial variability of the evolution of the three indicators over the domain is reported in Fig. 11, showing the distribution of the linear trends obtained over the 6 decades and their significance.

Despite the high spatial variability of trends as a consequence of the few points entering into the linear fit, the areas with the greatest and significant increase of indicator values are located in the north-western part and in a less extended portion in the eastern domain. These findings are in agreement with the spatial distribution of SPEI-3 trends over the study area even if in this case a more evident signal is depicted for the northernmost parts which turned out to be more influenced by variation in drought features.

CONCLUSIONS

The 1951–2017 monthly series of the two meteorological drought indices SPI and SPEI were computed and

analyzed for a portion of Po plain in northern Italy. The series were extracted from a gridded dataset of monthly precipitation and mean temperature records covering the study area at 30-arc second spatial resolution. The high-resolution fields were based on a quality checked and homogenized archive of long station records located on the domain and surrounding areas which were interpolated onto the grid by means of an anomaly-based method.

The long-term trend analysis on seasonal and annual SPI and SPEI areal series, which were computed by averaging the gridded precipitation and temperature records, pointed out a 5%-significant negative trend in summer for SPI ($-0.14 \text{ decade}^{-1}$) and in spring, summer and year for SPEI (-0.14 , -0.22 and $-0.17 \text{ decade}^{-1}$, respectively). Significant drying tendencies in both indices were depicted also over shorter time windows (20-30 years) starting in 1980 and in 1970 for spring and summer, respectively. In SPEI series the negative tendencies were more evident than in SPI values, probably due to the increasing role of evapotranspiration in recent decades triggered by warming conditions.

The gridded dataset allowed to investigate the long-term spatial variability of the drought indices over the domain. Significant negative trends occurred over the western portion of the study area for summer and annual SPI series and over the south-western parts for spring, sum-

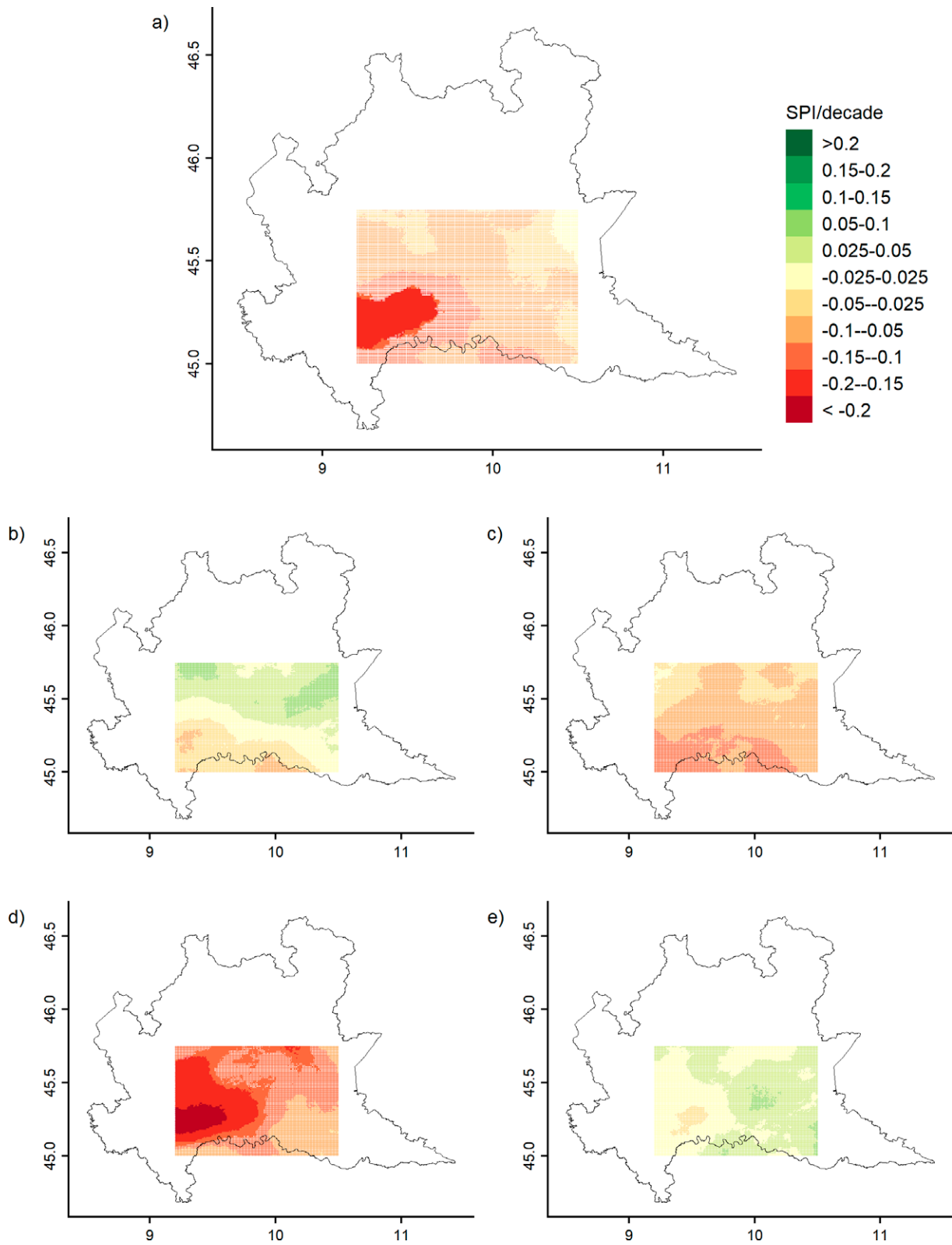


Fig. 6. Spatial distribution of TS trends for annual (a) and seasonal (winter b), spring c), summer d) and autumn e)) SPI series over the domain. Filled areas correspond to trends with MK p-values < 0.05, while dotted areas represent not significant trends. All values are expressed as index variation per decade.

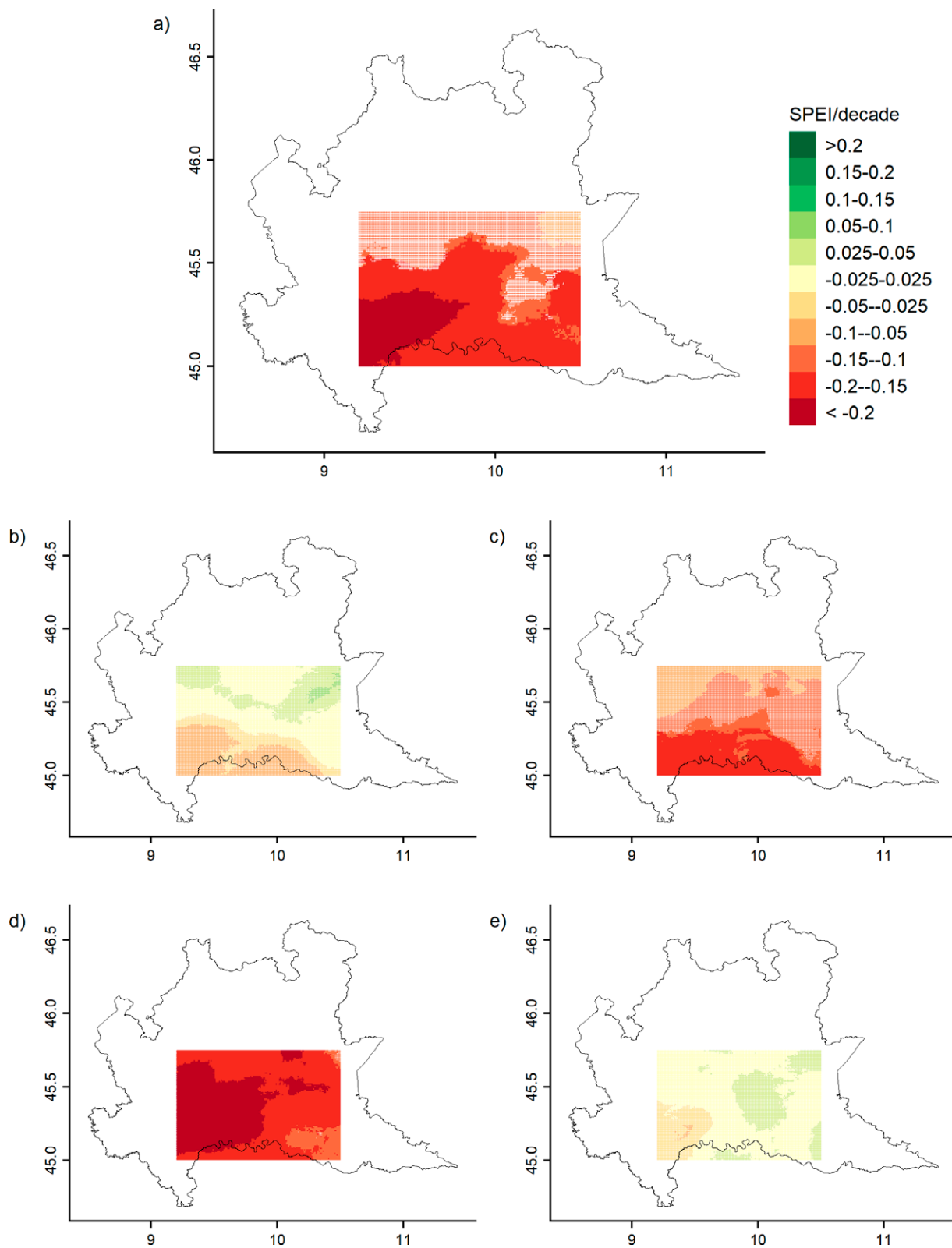


Fig. 7. Spatial distribution of TS trends for annual (a) and seasonal (winter b), spring c), summer d) and autumn e)) SPEI series over the domain. Filled areas correspond to trends with MK p-values < 0.05, while dotted areas represent not significant trends. All values are expressed as index variation per decade.

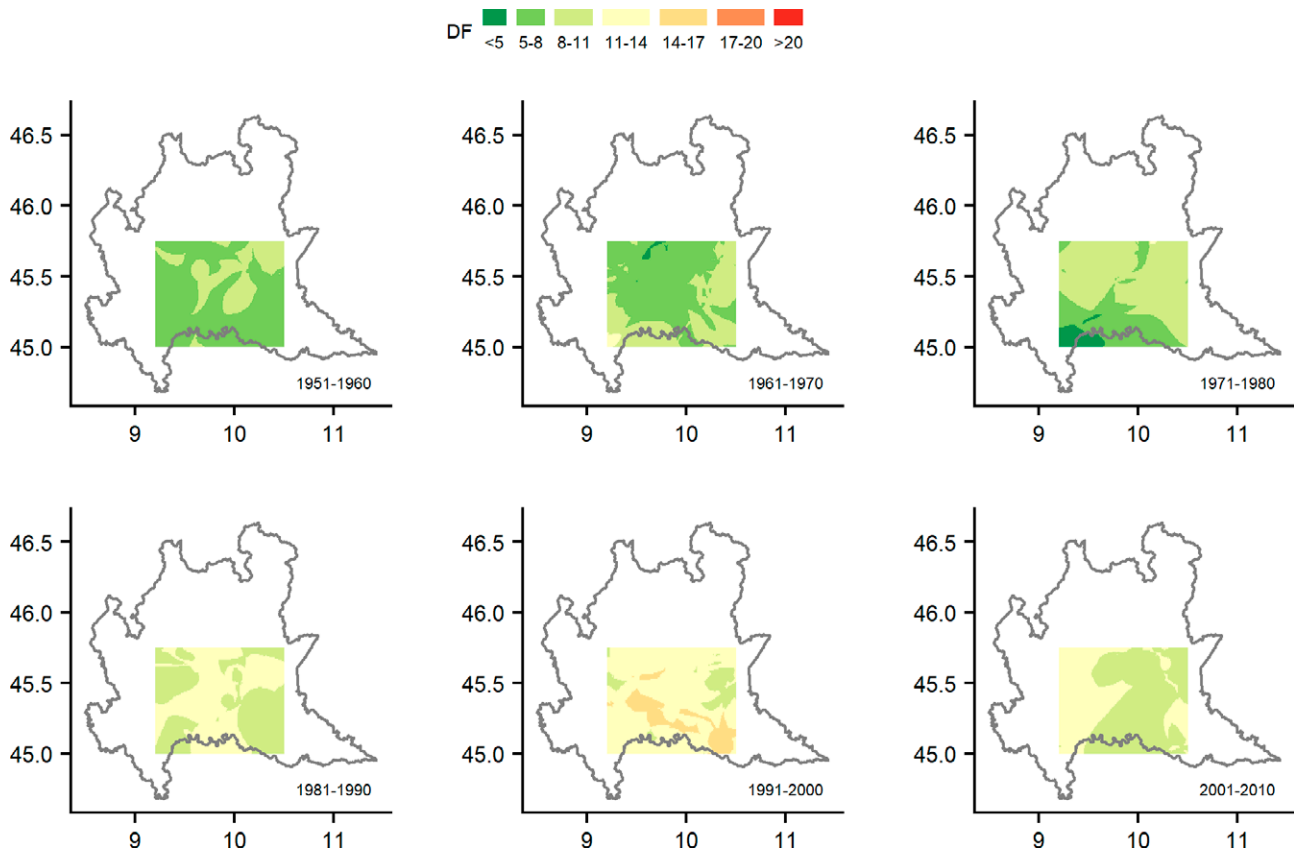


Fig. 8. Spatial distribution of the frequency of drought events (DF) identified in SPEI-3 series over subsequent decades.

mer and annual SPEI series, with the most relevant decrease ($< -0.2 \text{ decade}^{-1}$) in summer for both indices.

The drought spells identified in SPEI-3 over the domain for the whole 67-year period showed an overall intensification in terms of frequency, duration and severity from the 80's onwards. The linear trend analysis on the drought features for subsequent decades partly confirms the outcomes of trend assessment for the seasonal SPEI series, with the western part of the domain mostly affected by variations in drought indices, while the northern portion showed a greater sensitivity to the changes in drought features.

The spatio-temporal variability analysis of the two analyzed drought indices (SPI and SPEI) carried out for the central part of Lombardy plain suggests that the drought risk is expected to increase in the near future as a result of the climate change, leading to a decline in precipitation and an increase in air temperature, and consequently in crop evapotranspiration rates confirming the results of other studies for the same area (e.g. Crespi et al., 2021 and Ranzi et al., 2021). This will have impacts on irrigated agriculture, due to the combined effect of increasing crop water requirements and decreasing summer

flows in the rivers that supply water for irrigation, caused by reduced snow accumulation in winter and anticipated snow melting in spring (see e.g. Jenicek et al., 2018). This mismatch between crop water needs and river flows has already started to manifest itself in the last years increasing the risk of water scarcity (i.e. resources available for irrigation less than irrigation demand) during the months of higher irrigation needs for the majority of crops. This will happen also in geographic areas historically characterized by a good water availability for irrigation such as the Lombardy plain. Further analyses are addressed to forthcoming studies to evaluate more in detail the main factors explaining the spatial variability of drought index trends over the domain, and to extend the high-resolution drought characterization to a larger area in the Po plain. Moreover, the extension of the present study with the analysis of the future drought projections for the region from climate model scenarios would be essential to better evaluate how the drought risk is expected to evolve in the near and far future under climate change and this will be addressed in a forthcoming paper. The availability of detailed information on the drought evolution over northern Italy in the past, present and future could provide relevant

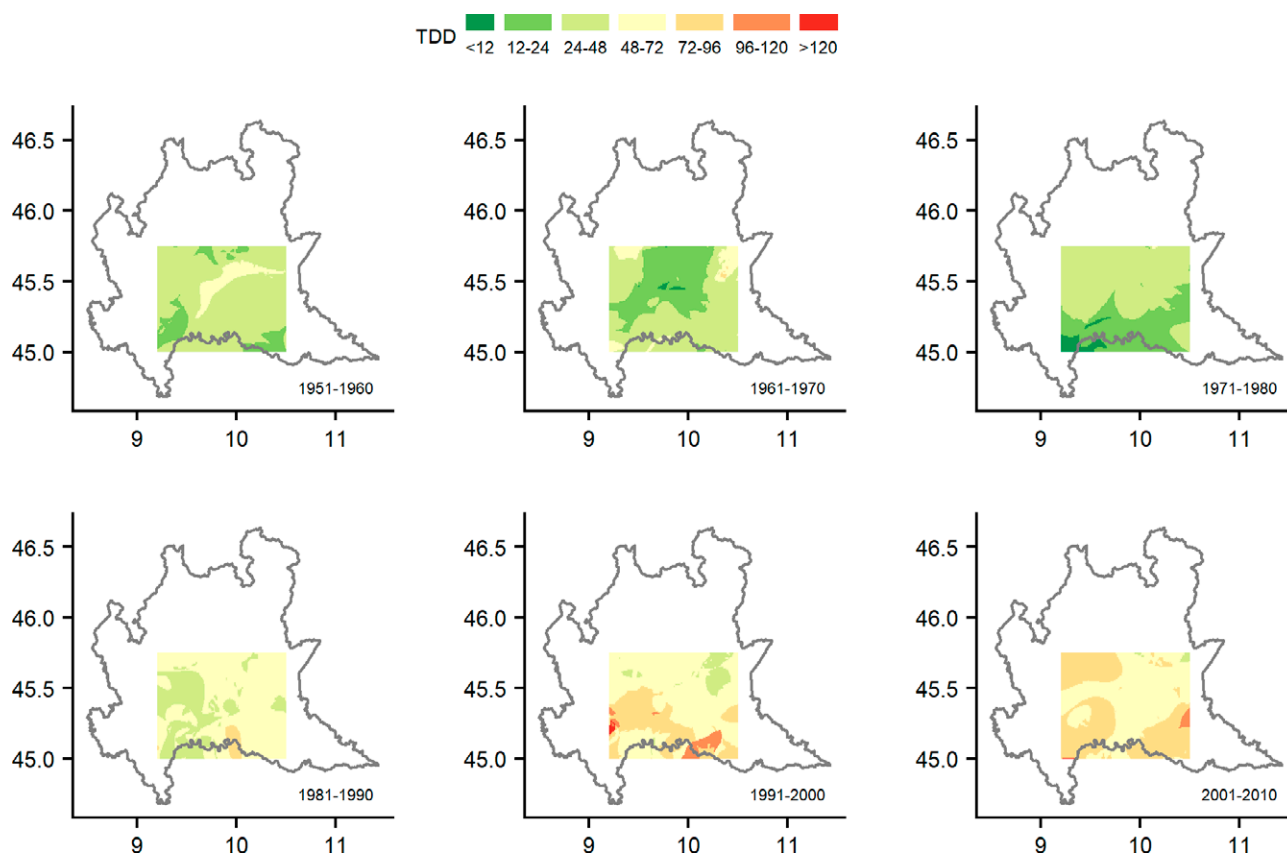


Fig. 9. Spatial distribution of the total month duration of drought events (TDD) identified in SPEI-3 series over subsequent decades.

supporting information to the management of current and future agricultural activities and production.

ACKNOWLEDGEMENTS

The support of Fondazione Cariplo through the So-Watch (Soft path water management adaptation to changing climate) project is gratefully acknowledged.

REFERENCES

- Allen R.G., Pereira L.S., Raes D., Smith M., 1998. Crop evapotranspiration – guidelines for computing crop water requirements. FAO Irrigation and drainage paper 56. Food and Agriculture Organization, Rome.
- Baronetti A., González-Hidalgo J.C., Vicente-Serrano S.M., Acquaotta F., Fratianni S., 2020. A weekly spatio-temporal distribution of drought events over the Po Plain (North Italy) in the last five decades. *International Journal of Climatology*, 40: 4463–4476. <https://doi.org/10.1002/joc.6467>
- Beguiería S., Vicente-Serrano S.M., Reig F., Latorre, B., 2014. Standardized precipitation evapotranspiration index (SPEI) revisited: parameter fitting, evapotranspiration models, tools, datasets and drought monitoring. *International Journal of Climatology*, 34: 3001–3023. <https://doi.org/10.1002/joc.3887>
- Bordi I., Sutera A., 2007. Drought Monitoring and Forecasting at Large Scale. In: Rossi G., Vega T., Bonaccorso B. (eds) *Methods and Tools for Drought Analysis and Management*. Water Science and Technology Library, vol 62. Springer, Dordrecht. https://doi.org/10.1007/978-1-4020-5924-7_1
- Briffa K.R., Van Der Schrier G., Jones P.D., 2009. Wet and dry summers in Europe since 1750: evidence of increasing drought. *International Journal of Climatology*, 29(13): 1894–1905. <https://doi.org/10.1002/joc.1836>
- Brunetti M., Maugeri M., Monti F., Nanni T., 2006. Temperature and precipitation variability in Italy in the last two centuries from homogenised instrumental time series. *International Journal of Climatology*, 26: 345–381. <https://doi.org/10.1002/joc.1251>
- Brunetti M., Lentini G., Maugeri M., Nanni T., Auer I., Böhm R., Schöner W., 2009. Climate variability and

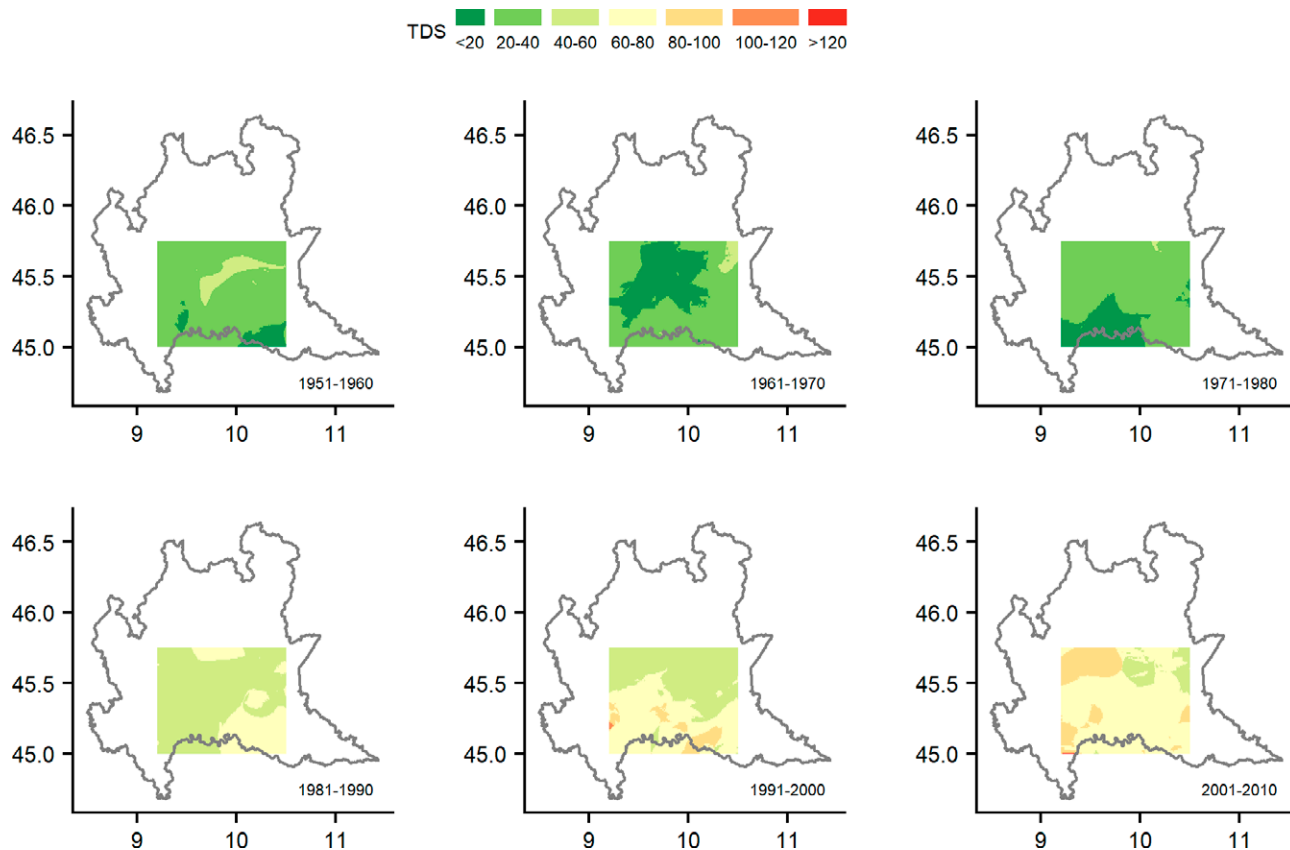


Fig. 10. Spatial distribution of the total severity of drought events (TDS) identified in SPEI-3 series over subsequent decades.

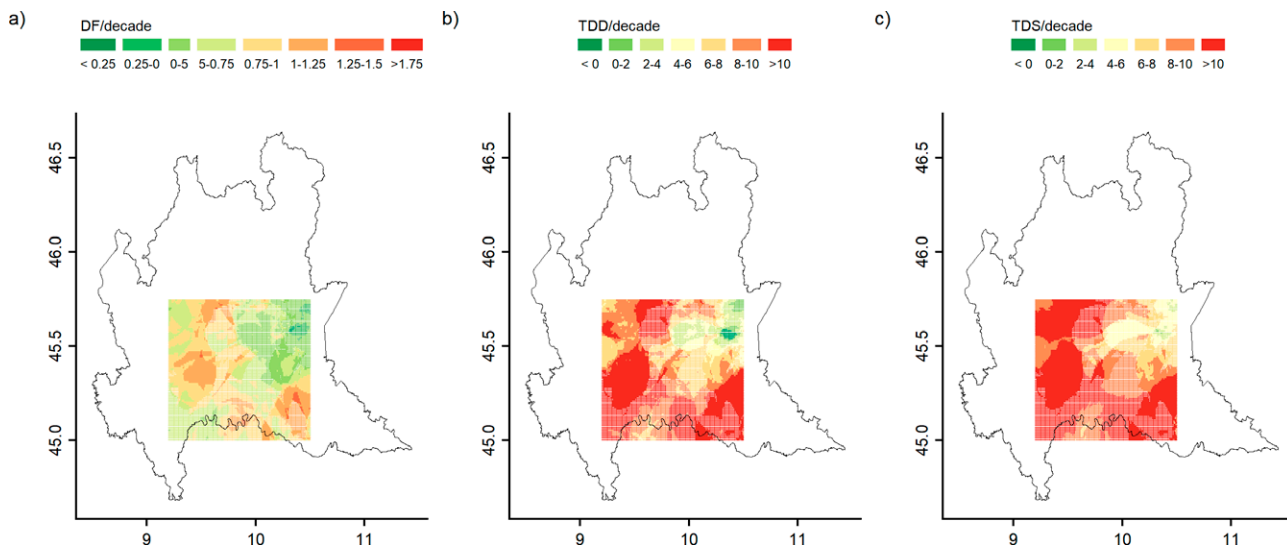


Fig. 11. Distribution of linear trend values of a) DF, b) TDD and c) TDS over 6 subsequent decades from 1951 to 2010 obtained from SPEI-3 series. Filled areas correspond to significant trends (p -value < 0.05), while grid cells corresponding to not significant trends are reported as dotted areas.

- change in the Greater Alpine Region over the last two centuries based on multi-variable analysis. *International Journal of Climatology*, 29: 2197–2225. <https://doi.org/10.1002/joc.1857>
- Brunetti M., Lentini G., Maugeri M., Nanni T., Simolo C., Spinoni J., 2012. Projecting North Eastern Italy temperature and precipitation secular records onto a high-resolution grid. *Physics and Chemistry of the Earth, parts A/B/C*, 40–41: 9–22. <https://doi.org/10.1016/j.pce.2009.12.005>
- Brunetti M., Maugeri M., Nanni T., Simolo C., Spinoni J., 2014. High-resolution temperature climatology for Italy: interpolation method intercomparison. *International Journal of Climatology*, 34: 1278–1296. <https://doi.org/10.1002/joc.3764>
- Buttafuoco G., Caloiero T., Coscarelli R., 2015. Analyses of Drought Events in Calabria (Southern Italy) Using Standardized Precipitation Index. *Water Resource Management*, 29: 557–573. <https://doi.org/10.1007/s11269-014-0842-5>
- Craddock J., 1979. Methods of comparing annual rainfall records for climatic purposes. *Weather*, 34: 332–346. <https://doi.org/10.1002/j.1477-8696.1979.tb03465.x>
- Crespi A., Brunetti M., Maugeri M., Ranzi R., Tomirotti M., 2018a. 1845–2016 gridded dataset of monthly precipitation over the upper Adda river basin: a comparison with runoff series. *Advances in Science and Research*, 15: 173–181. <https://doi.org/10.5194/asr-15-173-2018>
- Crespi A., Brunetti M., Lentini G., Maugeri M., 2018b. 1961–1990 high-resolution monthly precipitation climatologies for Italy. *International Journal of Climatology*, 38: 878–895. <https://doi.org/10.1002/joc.5217>
- Crespi A., Brunetti M., Ranzi R., Tomirotti M., Maugeri M., 2021. A multi-century meteo-hydrological analysis for the Adda river basin (Central Alps). Part I: Gridded monthly precipitation (1800–2016) records. *International Journal of Climatology*, 41: 162–180. <https://doi.org/10.1002/joc.6614>
- Dai A., Trenberth K.E., Qian T., 2004. A global dataset of Palmer Drought Severity Index for 1870–2002: relationship with soil moisture and effects of surface warming. *Journal of Hydrometeorology*, 5(6): 1117–1130. <https://doi.org/10.1175/JHM-386.1>
- Daly C., Gibson W.P., Taylor G.H., Johnson G.L., Pastoris, P., 2002. A knowledge-based approach to the statistical mapping of climate. *Climate Research*, 22: 99–113. <https://doi.org/10.3354/cr022099>
- Di Lena B., Vergni L., Antenucci F., Todisco F., Manocchi F., 2014. Analysis of drought in the region of Abruzzo (Central Italy) by the Standardized Precipitation Index. *Theoretical and Applied Climatology*, 115: 41–52. <https://doi.org/10.1007/s00704-013-0876-2>
- Foresti L., Sideris I., Panziera L., Nerini D., Germann U., 2018. A 10-year radar-based analysis of orographic precipitation growth and decay patterns over the Swiss Alpine region. *Quarterly Journal of the Royal Meteorological Society*, 144: 2277–2301. <https://doi.org/10.1002/qj.3364>
- Founda D., Varotsos K.V., Pierros F., Giannakopoulos C., 2019. Observed and projected shifts in hot extremes' season in the Eastern Mediterranean. *Global and Planetary Change*, 175, 190–200. <https://doi.org/10.1016/j.gloplacha.2019.02.012>
- IPCC, 2014. Summary for Policymakers. In: *Climate Change 2014: Mitigation of Climate Change. Contribution of Working Group III to the Fifth Assessment Report of the Intergovernmental Panel on Climate Change* [Edenhofer, O., R. Pichs-Madruga, Y. Sokona, E. Farahani, S. Kadner, K. Seyboth, A. Adler, I. Baum, S. Brunner, P. Eickemeier, B. Kriemann, J. Savolainen, S. Schlömer, C. von Stechow, T. Zwickel and J.C. Minx (eds.)]. Cambridge University Press, Cambridge, United Kingdom and New York, NY, USA. <https://doi.org/10.1017/cbo9781107415416.005>
- Isotta F.A., Frei C., Weilguni V., Perčec Tadić M., Lassègues P., Rudolf B., Pavan V., Cacciamani C., Antolini G., Ratto S.M., Munari M., Micheletti S., Bonati V., Lussana C., Ronchi C., Panettieri E., Mariogo G., Vertaničk G., 2014. The climate of daily precipitation in the Alps: development and analysis of a high-resolution grid dataset from pan-Alpine rain-gauge data. *International Journal of Climatology*, 34: 1657–1675. <https://doi.org/10.1002/joc.3794>
- Kendall M.G., 1975. *Rank Correlation Methods*. Griffin, London.
- Lionello P., Scarascia L., 2018. The relation between climate change in the Mediterranean region and global warming. *Regional Environmental Change*, 18: 1481–1493. <https://doi.org/10.1007/s10113-018-1290-1>
- McKee T.B., Doeskin N.J., Kleist J., 1993. The relationship of drought frequency and duration to time scales. In *Proceedings of the 8th Conference on Applied Climatology*. American Meteorological Society: 179–184.
- Mitchell T.D., Jones P.D., 2005. An improved method of constructing a database of monthly climate observations and associated high resolution grids. *International Journal of Climatology*, 25: 693–712. <https://doi.org/10.1002/joc.1181>
- New M., Todd M., Hulme M., Jones P., 2001. Precipitation measurements and trends in the twentieth century. *International Journal of Climatology*, 21: 1899–1922. <https://doi.org/10.1002/joc.680>
- Parsons D.J., Rey D., Tanguy M., Holman I.P., 2019. Regional variations in the link between drought indi-

- ces and reported agricultural impacts of drought. *Agricultural Systems*, 173:119–129. <https://doi.org/10.1016/j.agsy.2019.02.015>
- Piccarreta M., Capolongo D., Boenzi F., 2004. Trend analysis of precipitation and drought in Basilicata from 1923 to 2000 within a southern Italy context. *International Journal of Climatology*, 24: 907–922. <https://doi.org/10.1002/joc.1038>
- Ranzi R., Michailidi E.M., Tomirotti M., Crespi A., Brunetti M., Maugeri M., 2021. A multi-century meteorological analysis for the Adda river basin (Central Alps). Part II: Daily runoff (1845–2016) at different scales. *International Journal of Climatology*, 41: 181–199. <https://doi.org/10.1002/joc.6678>
- Sen P.K., 1968. Estimates of the regression coefficient based on Kendall's tau. *Journal of the American Statistical Association*, 63(324): 1379–1389. <https://doi.org/10.2307/2285891>
- Spinoni J., Naumann G., Carrao H., Barbosa P., Vogt J., 2014. World drought frequency, duration, and severity for 1951–2010. *International Journal of Climatology*, 34(8): 2792–2804. <https://doi.org/10.1002/joc.3875>
- Spinoni J., Naumann G., Vogt J., 2015. Spatial patterns of European droughts under a moderate emission scenario. *Advances in Science and Research*, 12(1): 179–186. <https://doi.org/10.5194/asr-12-179-2015>
- Spinoni J., Vogt J.V., Naumann G., Barbosa P., Dosio A., 2018. Will drought events become more frequent and severe in Europe?. *International Journal of Climatology*, 38: 1718–1736. <https://doi.org/10.1002/joc.5291>
- Stagge J.H., Kohn I., Tallaksen L.M., Stahl K., 2015. Modeling drought impact occurrence based on meteorological drought indices in Europe. *Journal of Hydrology*, 530: 37–50. <https://doi.org/10.1016/j.jhydrol.2015.09.039>
- Stagge J.H., Kingston D.G., Tallaksen L.M., Hannah D.M., 2017. Observed drought indices show increasing divergence across Europe. *Scientific Reports*, 7: 14045. <https://doi.org/10.1038/s41598-017-14283-2>
- Theil H., 1950. A rank-invariant method of linear and polynomial regression analysis. I. *Proceedings of the Koninklijke Nederlandse Akademie van Wetenschappen A53*: 386–392.
- Thorntwaite C.W., 1948. An approach toward a rational classification of climate. *Geographical Review*, 38: 55–94. <https://doi.org/10.2307/210739>
- Vergni L., Todisco F., 2011. Spatio-Temporal Variability of Precipitation, Temperature and Agricultural Drought Indices in Central Italy. *Agricultural and Forest Meteorology*, 151: 301–313. <https://doi.org/10.1016/j.agrformet.2010.11.005>
- Vicente-Serrano S.M., Beguería S., López-Moreno J.I., 2010. A Multiscalar Drought Index Sensitive to Global Warming: The Standardized Precipitation Evapotranspiration Index. *Journal of Climate*, 23: 1696–1718. <https://doi.org/10.1175/2009JCLI2909.1>
- Vicente-Serrano S.M., Beguería S., Lorenzo-Lacruz J., Camarero J. J., López-Moreno J. I., Azorin-Molina C., Revuelto J., Morán-Tejeda E., Sanchez-Lorenzo A., 2012. Performance of Drought Indices for Ecological, Agricultural, and Hydrological Applications. *Earth Interactions*, 16:1–27. <https://doi.org/10.1175/2012EI000434.1>
- Vicente-Serrano S.M., Lopez-Moreno J.I., Beguería S., Lorenzo-Lacruz J., Sanchez-Lorenzo A., García-Ruiz J. M., Azorin-Molina C., Moran-Tejeda E., Revuelto J., Trigo R., Coelho F., Espejo F., 2014. Evidence of increasing drought severity caused by temperature rise in southern Europe. *Environmental Research Letters*, 9(4): 044001. <https://doi.org/10.1088/1748-9326/9/4/044001>